THE JOURNAL OF PHYSICAL CHEMISTRY B LETTERS

2006, *110,* 655−658
Published on Web 12/22/2005

Understanding Hydrogen Adsorption in Metal−Organic Frameworks with Open Metal Sites: A Computational Study

Qingyuan Yang and Chongli Zhong*

Department of Chemical Engineering, Beijing University of Chemical Technology, Beijing 100029, China

Received: October 15, 2005; In Final Form: December 4, 2005

Recent experimental investigations show that the open metal sites may have a favorable impact on the hydrogen adsorption capacity of metal−organic frameworks (MOFs); however, no definite evidence has been obtained to date and little is known on the interactions between hydrogen and the pore walls of this kind of MOFs. In this work, a combined grand canonical Monte Carlo simulation and density functional theory calculation is performed on the adsorption of hydrogen in MOF-505, a recently synthesized MOF with open metal sites, to provide insight into molecular-level details of the underlying mechanisms. This work shows that metal−oxygen clusters are preferential adsorption sites for hydrogen, and the strongest adsorption of hydrogen is found in the directions of coordinatively unsaturated open metal sites, providing evidence that the open metal sites have a favorable impact on the hydrogen sorption capacity of MOFs. The storage capacity of hydrogen of MOF-505 at room temperature and moderate pressures is predicted to be low, in agreement with the outcome for hydrogen physisorption in other porous materials.

Hydrogen has received much attention as a pollution-free energy source. A safe and efficient storage system is crucial for the future wide utilization of hydrogen in vehicles and portable electronics. Although various materials have been studied as hydrogen-storage materials, none are capable of meeting the U.S. Department of Energy (DOE) cost and performance targets yet. Due to their amenability to design and fine-tunable pore structures, metal−organic frameworks (MOFs) have been considered for this application[1−5] and various MOFs have been synthesized and characterized for their hydrogen-storage capacities.[6−11] Although several quantum chemical calculations[12−15] and molecular simulations[15−18] have been performed, knowledge on the interactions between hydrogen and the pore walls of MOFs is still less than satisfying. Furthermore, to the best of our knowledge, no computational studies have been carried out on hydrogen adsorption in MOFs with open metal sites that have shown enhanced hydrogen-storage capacity experimentally; thus, in this work, a computational study is performed to give insight into molecular-level details of the underlying mechanisms.

To understand the role of the open metal sites on hydrogen adsorption in MOFs, density functional theory (DFT) calculations were performed using DMol[3] as implemented in the Materials Studio package.[19] We used DFT with the PBE exchange-correlation functional for all of our calculations (see the Supporting Information). This method has been used to study the adsorption sites of hydrogen in MOF-5 successfully.[12] In this work, the MOF-505 synthesized by Chen al.[20] was selected as a representative of MOFs with open metal sites. The structural model was constructed from the X-ray diffraction (XRD) data given by Chen et al.,[20] as shown in Figure 1. MOF-505 has an overall 3-periodic network consisting of two kinds of pores (see Figure 1a and b). The smaller pore in MOF-505 is defined by six inorganic $Cu_2(CO_2)_4$ units, and the larger pore, by six organic bptc^{4-} (3,3′,5,5′-biphenyltetracarboxylic group) units. In addition, $Cu_2(CO_2)_4$ has a paddle wheel structure, and the open metal sites are located at Cu atoms along the directions of paddle wheel axes which are coordinatively unsaturated.

In our calculations, several locations and orientations were tested around the inorganic $Cu_2(CO_2)_4$ unit in MOF-505. The strongest adsorption configuration was found to locate in the direction of open metal sites with an adsorption energy (with respect to gas phase hydrogen) of −13.44 kJ/mol, the close-up view of which is shown in Figure 2a. When hydrogen was located in the direction of the Cu−Cu axis, as shown in Figure 2b, the adsorption energy dropped down to −9.71 kJ/mol. This illustrates that the hydrogen molecule is inclined to expose the negative lobe of its quadrupole (a torus around the bond axis) to the Cu atoms.[13] We also determined the adsorption configurations of a hydrogen molecule around the equatorial quadrant defined by adjacent carboxylate groups of paddle wheel $Cu_2(CO_2)_4$, as shown in Figure 2c and d. The adsorption energy for hydrogen perpendicular to the paddle wheel axis (i.e., Cu−Cu axis) is −10.25 kJ/mol, as shown in Figure 2c. This is the most stable configuration other than those in the directions of the open metal sites (Figure 2a). Obviously, the adsorption energy in the direction of the open metal sites is larger by about 30% than those positions far from the open metal sites, indicating that the open metal sites have a favorable impact on the hydrogen adsorption capacity in MOF-505. This gives direct evidence to the experimental observations of Chen et al.[20] and Kaye and Long,[21] leading to a molecular-level understanding of the role of the open metal sites on hydrogen adsorption in MOFs.

To understand the pressure dependence of hydrogen adsorption behavior in MOF-505, grand canonical Monte Carlo

* Corresponding author. E-mail: zhongcl@mail.buct.edu.cn.

10.1021/jp055908w CCC: $33.50

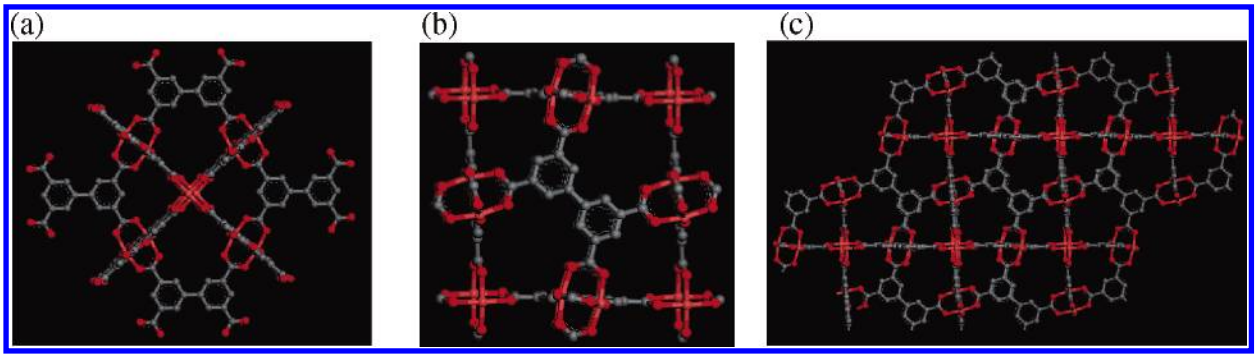

Figure 1. Single-crystal X-ray structure of MOF-505, [Cu_2(bptc)]: (a) smaller pore in MOF-505 defined by six inorganic $Cu_2(CO_2)_4$ units (representing the faces of a cubic NbO subunit); (b) larger pore in MOF-505 defined by six organic $bptc^{4-}$ units (again representing the faces of a cubic NbO subunit); (c) supercell of MOF-505 consisting of 2 × 2 × 1 unit cells (Cu, orange; O, red; C, gray, and H atoms are omitted for clarity).

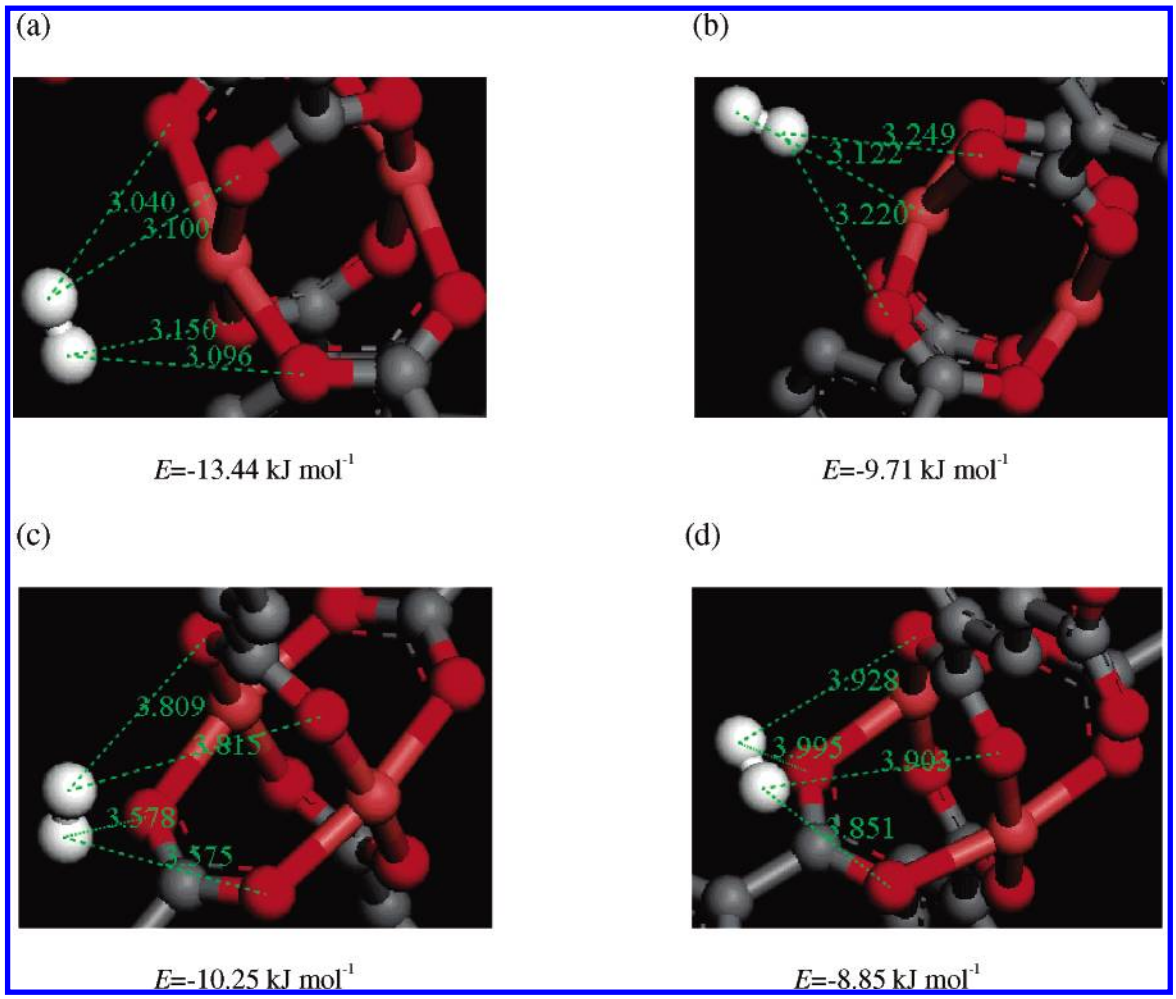

Figure 2. Close-up view of the DFT calculated configurations of an adsorbed hydrogen molecule around the inorganic $Cu_2(CO_2)_4$ unit in MOF-505: (a) hydrogen adsorbed perpendicularly in the direction of the open metal sites; (b) hydrogen adsorbed parallel in the direction of the open metal sites; (c and d) hydrogen adsorbed not in the direction of the open metal sites (Cu, orange; O, red; C, gray; hydrogen, white).

(GCMC) simulations[18,22] were further performed to predict adsorption isotherms (see the Supporting Information). Since the effect of electrostatic potential on hydrogen adsorption in MOFs is very significant at low coverage,[16] the atomic partial charges of the MOF-505 framework were taken into account, which were computed from the popular electrostatic potentials (ChelpG) method, based on DFT calculation using the unrestricted B3LYP functional. Calculation details and the corresponding calculated results are described in the Supporting Information. In the GCMC simulations, the hydrogen molecule was treated as a diatomic molecule modeled by a Lennard-Jones (LJ) core located at the center of mass and three partial charges with two located at hydrogen atoms and one at the center between two hydrogen atoms. Since the quantum effect is important for hydrogen adsorption at low temperature, the quadratic Feynman-Hibbs (FH) effective potential[23,24] was adopted to calculate all of the LJ interactions to take into account the quantum effect (see the Supporting Information). The interactions of hydrogen with the atoms of MOF-505 were described by the all-atom OPLS force field (OPLS-AA).[25] To better represent the experimental adsorption isotherm of hydrogen in MOF-505 at 77 K (see Figure 3a),[19] the energy parameters for oxygen and copper were refitted (see the Supporting Information). The Ewald summation method[22] was

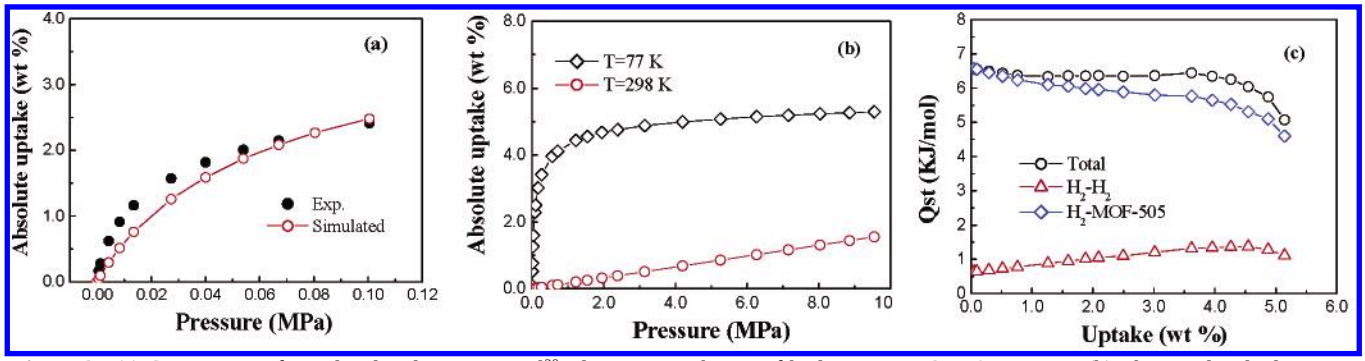

Figure 3. (a) Comparison of simulated and experimental[20] adsorption isotherms of hydrogen in MOF-505 at 77 K. (b) The simulated adsorption isotherms of hydrogen in MOF-505 at 77 and 298 K with $P = 0-10$ MPa. (c) The simulated isosteric heat of adsorption for hydrogen in MOF-505 at 77 K. The H_2-H_2 (triangles) and H_2-MOF-505 (diamonds) contributions to the total heat curve (circles) are shown.

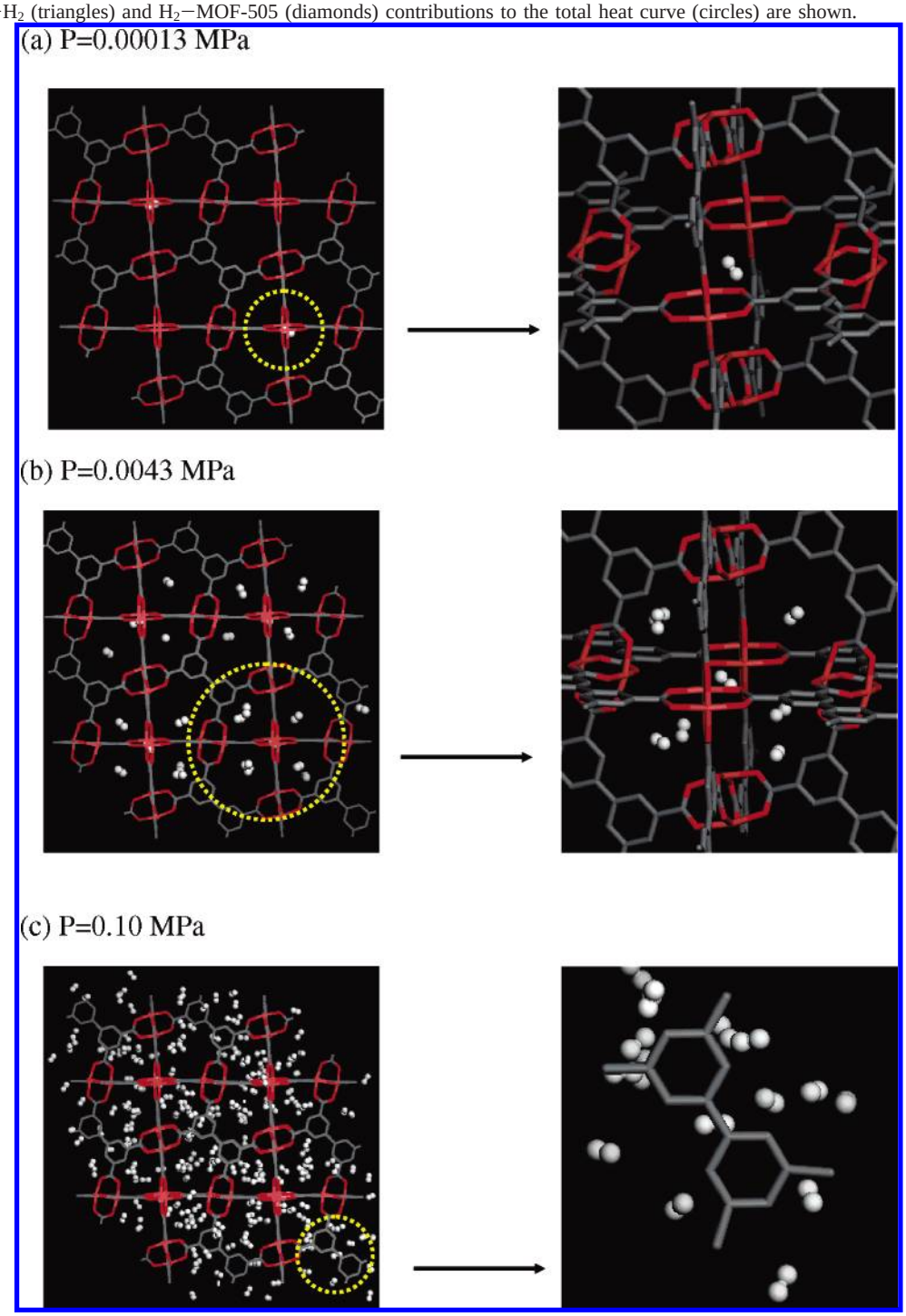

Figure 4. Snapshots of the structures of MOF-505 with adsorbed hydrogen at various pressures (the MOF-505 framework is shown in line style with color: Cu, orange; O, red; C, gray; hydrogen, white spheres).

employed to calculate the electrostatic interactions betweenhydrogen molecules as well as between hydrogen molecules and the MOF-505 framework.

To investigate the adsorption mechanism as well as the effects of pressure on hydrogen adsorption in MOF-505, GCMC simulations were performed at $T = 77$ and 298 K, respectively, in the pressure range $P = 0-10.0$ MPa. Although the hydrogen uptake in MOF-505 at 77 K and 0.1 MPa is 2.47 wt %, much higher than that of other MOFs studied in previous work,[18] such as MOF-5 (1.32 wt %),[11] the simulated maximum hydrogen uptake in MOF-505 at 77 K is 5.60 wt %, much lower than that in MOF-5 (10.0 wt %).[18] This is mainly caused by the fact that MOF-505 has a much smaller free volume and higher crystal density than MOF-5. Therefore, it is clear that although open metal sites can enhance hydrogen adsorption capacity at low pressures, other properties such as free volume play an important role at high pressures. As a result, to design a MOF material that has a high hydrogen-storage capacity, all of these factors have to be taken into account and combined properly. On the other hand, Figure 3b shows that, at room temperature and $P = 5$ MPa, the simulated uptake of hydrogen in MOF-505 is only 0.82 wt %, similar to that in MOF-5 (0.73 wt %).[11] Simulations on other porous materials, such as single-walled carbon nanotube (SWNT) arrays (0.45 wt %)[26] and Na-LSX zeolite (0.69 wt %),[27] also show that porous materials cannot store appreciable amounts of hydrogen at room temperature and moderate pressures, illustrating that the practical applications of porous materials as hydrogen-storage materials is unlikely to be possible with materials of this sort.

In addition, the loading dependence of the isosteric heat of adsorption for hydrogen in MOF-505 at 77 K was simulated, as shown in Figure 3c, where the contributions from both the H_2-H_2 and H_2-MOF-505 are given. The isosteric heat of adsorption decreases with increasing hydrogen loading; this is consistent with the fact that the binding energies of hydrogen are heterogeneous in the pores and hydrogen molecules first occupy lower energy configurations, leading to larger isosteric heats of adsorption at lower loadings.

Furthermore, the snapshots of the structures of MOF-505 with adsorbed hydrogen at various pressures were examined, and some typical ones are given in Figure 4. A careful examination of the snapshots obtained show that the mechanism of hydrogen adsorption in MOF-505 is the following: hydrogen molecules first occupy the center regions of the smaller pores defined by six inorganic $Cu_2(CO_2)_4$ units (Figure 4a); with increasing pressure, they begin to be adsorbed at the corners of the larger pores (the intersectional pockets between the smaller and larger pores formed by three inorganic $Cu_2(CO_2)_4$ units) (Figure 4b); with further increasing pressure, hydrogen molecules are adsorbed mainly around the organic units. This work, together with our previous simulations on MOF-5[18] and the experimental observations,[6,8] shows that all of the MOFs behave similarly upon hydrogen adsorption; that is, clusters of inorganic units are the most preferential hydrogen adsorption sites in MOFs.

In summary, the combined DFT and GCMC simulation study of this work shows that open metal sites give favorable impact on the hydrogen adsorption in MOFs at low pressures, while, at high pressures, other material properties such as free volume play an important role. Therefore, to have a high hydrogen-storage capacity, a MOF material should incorporate the advantages of having open metal sites, with a large free volume, low crystal density, and suitable pore size. In addition, this work shows that MOFs cannot store appreciable amounts of hydrogen at room temperature and moderate pressures, which is also the case for other porous materials such as carbon nanotubes and zeolites. Therefore, the practical application of porous materials as hydrogen-storage materials by the physisorption approach is unlikely to be possible.

Acknowledgment. The financial support from the Natural Science Foundation of China (Contract: 20476003) and the Specialized Research Fund for the Doctoral Program of Higher Education of China (Contract: 20040010002) is greatly appreciated.

Supporting Information Available: Details of DFT calculations, simulations, and force field parameters. This material is available free of charge via the Internet at http://pubs.acs.org.

References and Notes

(1) Rowsell, J. C. L.; Yaghi, O. M. *Angew. Chem., Int. Ed.* **2005**, *44*, 4670−4679.
(2) Snurr, R. Q.; Hupp, J. T.; Nguyen, S. T. *AIChE J.* **2004**, *50*, 1090−1094.
(3) Seayad, A. M.; Antonelli D. M. *Adv. Mater.* **2004**, *16*, 765−777.
(4) Rosseinsky, M. J. *Microporous Mesoporous Mater.* **2004**, *73*, 15−30.
(5) Rowsell, J. L. C.; Yaghi, O. M. *Microporous Mesoporous Mater.* **2004**, *73*, 3−14.
(6) Rosi, N. L.; Eckert, J.; Eddaoudi, M.; Vodak, D. T.; Kim, J.; O'Keeffe, M.; Yaghi, O. M. *Science* **2003**, *300*, 1127−1129.
(7) Kesanli, B.; Cui, Y.; Smith, M. R.; Bittner, E. W.; Bockrath, B. C.; Lin, W. *Angew. Chem., Int. Ed.* **2005**, *44*, 72−75.
(8) Kubota, Y.; Takata, M.; Matsuda, R.; Kitaura, R.; Kitagawa, S.; Kato, K.; Sakata, M.; Kobayashi, T. C. *Angew. Chem., Int. Ed.* **2005**, *44*, 920−923.
(9) Dybtsev, D. N.; Chun, H. C.; Yoon, S. H.; Kim, D.; Kim, K. *J. Am. Chem. Soc.* **2004**, *126*, 32−33.
(10) Pan, L.; Sander, M. B.; Huang, X.; Li, J.; Smith, M.; Bittner, E.; Bockrath, B.; Johnson, J. K. *J. Am. Chem. Soc.* **2004**, *126*, 1308−1309.
(11) Rowsell, J. L. C.; Millward, A. R.; Park, K. S.; Yaghi, O. M. *J. Am. Chem. Soc.* **2004**, *126*, 5666−5667.
(12) Mueller, T.; Ceder, G. *J. Phys. Chem. B* **2005**, *109*, 17974−17983.
(13) Bordiga, S.; Vitillo, J. G.; Ricchiardi, G.; Regli, L.; Cocina, D.; Zecchina, A.; Arstad, B.; Bjørgen, M.; Hafizovic, J.; Lillerud, K. P. *J. Phys. Chem. B* **2005**, *109*, 18237−18242.
(14) Sagara, T.; Klassen, J.; Ortony, J.; Ganz, E. *J. Chem. Phys.* **2005**, *123*, 014701(1-4).
(15) Sagara, T.; Klassen, J.; Ganz, E. *J. Chem. Phys.* **2004**, *121*, 12543−12547.
(16) Garberoglio, G.; Skoulidas, A. I.; Johnson, J. K. *J. Phys. Chem. B* **2005**, *109*, 13094−13103.
(17) Skoulidas, A. I.; Sholl, D. S. *J. Phys. Chem. B* **2005**, *109*, 15760−15768.
(18) Yang, Q. Y.; Zhong, C. L. *J. Phys. Chem. B* **2005**, *109*, 11862−11864.
(19) *Accelrys, Inc., Materials Studio, 3.0 V*; Accelrys, Inc.: San Diego, CA, 2003.
(20) Chen, B. L.; Ockwig, N. W.; Millward, A. R.; Contreras, D. S.; Yaghi, O. M. *Angew. Chem., Int. Ed.* **2005**, *44*, 4745−44749.
(21) Kaye, S. S.; Long, J. R. *J. Am. Chem. Soc.* **2005**, *127*, 6506−6507.
(22) Frenkel, D.; Smit, B. *Understanding Molecular Simulation: From Algorithms to Applications*; Academic Press: San Diego, CA, 2002.
(23) Darkrim, F.; Levesque, D. *J. Phys. Chem. B* **2000**, *104*, 6773−6776.
(24) Tanaka, H.; Kanoh, H.; Yudasaka, M.; Iijima, S.; Kaneko, K. *J. Am. Chem. Soc.* **2005**, *127*, 7511−7516.
(25) Jorgensen, W. L.; Maxwell, D. S.; Tirado-Rives, J. *J. Am. Chem. Soc.* **1996**, *118*, 11225−11236.
(26) Wang, Q. Y.; Johnson, J. K. *J. Chem. Phys.* **1999**, *110*, 577−586.
(27) Weinberger, B.; Lamari, F. D.; Kayiran, B.; Gicquel, A.; Levesque. D. *AIChE J.* **2005**, *51*, 142−148.